

K^+ and π^+ momentum spectra from 2.5–3.1 GeV/c protons on carbon and two-body final-state spectral peaks from (p, K^+) and (p, π^+) reactions*

T. Bowen, D. A. DeLise, and A. E. Pifer

Department of Physics, University of Arizona, Tucson, Arizona 85721

(Received 9 October 1975)

A partially separated 0.9–1.8 GeV/c K^+ beam at the Bevatron was utilized as a spectrometer (0.9% full width at half maximum) to study the K^+ and π^+ momentum spectra at 0° from carbon and other target elements bombarded by 2.5–3.1 GeV/c protons. Searches were made for possible spectral peaks resulting from two-body final state reactions such as $^{12}\text{C}(p, K^+)^{13}\text{C}_\Lambda$ and $^{12}\text{C}(p, \pi^+)^{13}\text{C}$. Spectral peaks observed from $p(p, \pi^+)d$ assisted in calibrating the apparatus, and a spectral structure attributed to $p[p, K^+](p\Lambda)^*$ was observed, where $(p\Lambda)^*$ represents p and Λ with low relative momentum. No other K^+ or π^+ spectral peaks appeared above background; upper limits are given which this experiment places on $(d\sigma/d\Omega)_{\text{c.m.}}$ at 0° . The K^+ and π^+ momentum spectra at 0° from carbon bombarded by 2.50, 2.70, 2.89, and 3.10 GeV/c protons are also given.

NUCLEAR REACTIONS Hypernuclei $p(p, K^+)(p\Lambda)^*$, $E = 1.9\text{--}2.3$ GeV; measured $\sigma(E; \theta = 0)$ near maximum K^+ momentum; results poorly fitted by Goldberger-Watson type calculation of $p\text{--}\Lambda$ final state interaction. $^{12}\text{C}(p, K^+)$, $^{12}\text{C}(p, \pi^+)$, $E = 1.7\text{--}2.3$ GeV; measured $\sigma(E; \theta = 0, P)$. $^{12}\text{C}(p, \pi^+)^{13}\text{C}$, $^{12}\text{C}(p, K^+)^{13}\text{C}_\Lambda$, $^9\text{Be}(p, K^+)\text{--}^{10}\text{Be}_\Lambda$, $^{56}\text{Fe}(p, K^+)^{57}\text{Fe}_\Lambda$, $E = 1.7$ GeV; $d(p, K^+)^3\text{H}_\Lambda$, $E = 1.9$ GeV; $^{12}\text{C}(p, K^+)^{13}\text{C}$, $E = 1.9, 2.1$ GeV; searched and set upper limits on $\sigma(E; \theta = 0)$; deduced qualitative upper limit to high momentum components of Λ in $^{13}\text{C}_\Lambda$.

The attention of one of the authors was first drawn to $^AZ(p, K^+)^{A+1}Z_\Lambda$ reactions by the possibility that an accelerator such as LAMPF, which has insufficient proton energy to produce kaons in $p\text{--}p$ collisions, could produce them via reactions such as the above.¹ However, the authors became actively interested in studying these reactions in connection with feasibility studies of employing Bevatron heavy ion beams to make relativistically moving hypernuclei. Since hypernuclei moving with relativistic velocities could travel many centimeters before decaying, it might then be possible to study them with a wider variety of techniques than in the past. The simplest way (and the most ideal for experimenters because of the tight kinematic constraints) of producing hypernuclei with a beam of relativistically moving AZ ions might be:

$$^AZ(\text{projectile}) + p(\text{target}) \rightarrow ^{A+1}Z_\Lambda(\text{relativistic}) + K^+(\text{slow}). \quad (1)$$

In order to more precisely assess the feasibility of producing and selecting hypernuclei by means of Eq. (1), information was needed on $(d\sigma/d\Omega)_{\text{c.m.}}$ at 0° , where the three-momentum transfer from nucleus AZ to hypernucleus $^{A+1}Z_\Lambda$ is a minimum. These data were more readily obtainable by reversing the roles of projectile and target and studying with a counter experiment the reaction:

$$p(\text{projectile}) + ^AZ(\text{target}) \rightarrow K^+(\text{relativistic}) + ^{A+1}Z_\Lambda(\text{slow}). \quad (2)$$

For bombarding momenta available in Bevatron heavy ion acceleration (up to ~ 2.8 GeV/nucleon),² the K^+ in Eq. (2) would have momenta in the range 1.0–1.8 GeV/c, well suited for detection in an already existing partially separated K^+ beam line. The K^+ mesons from Eq. (2) at 0° in the laboratory would have a unique momentum depending upon the incident proton momentum and the masses of the particles, so they would be observed as a spectral peak or enhancement in the broad momentum spectrum of kaons produced in many-body final states.

If a spectral peak were observed, the momentum at which it occurred would provide a determination of the binding energy of the hypernucleus which was produced in association with the kaon. The spectral peak from the well studied $p(p, \pi^+)d$ reaction was ideally suited to calibrate the apparatus in two respects: (1) The position and width of the π^+ peak for several incident proton momenta would accurately calibrate the absolute momentum settings and resolution of the apparatus. (2) The flux of π^+ 's observed in the peaks could serve to calibrate the solid angle acceptance of the beam. It is an unusual coincidence in nature that for the proton momentum region of interest in this work

the π^+ momentum from $p(p, \pi^+)d$ almost exactly equals the K^+ momentum expected from $^{12}\text{C}(p, K^+)^{13}\text{C}_\Lambda$. The π^+ line is produced with $(d\sigma/d\Omega)_{\text{c.m.}} \approx 10 \mu\text{b/sr}$ in the region of interest, and it appeared feasible to detect the K^+ down to $(d\sigma/d\Omega)_{\text{c.m.}} \approx 10^{-3} \mu\text{b/sr}$.

A theoretical estimate of $(d\sigma/d\Omega)_{\text{c.m.}}$ in a process such as $^{12}\text{C}(p, K^+)^{13}\text{C}_\Lambda$ is extremely sensitive to the amplitude of high momentum components of the Λ wave function in $^{13}\text{C}_\Lambda$. Unfortunately, the kinematics of the reaction constrain the three-momentum transfer between ^{12}C and $^{13}\text{C}_\Lambda$, as viewed in the $^{13}\text{C}_\Lambda$ center-of-mass system, to be $\geq 0.965 \text{ GeV}/c$, which is large compared to characteristic momentum components $\approx 0.14 \text{ GeV}/c$, in nuclei. Using harmonic oscillator wave functions, Fetisov *et al.*³ estimate $(d\sigma/d\Omega)_{\text{c.m.}} \approx 10^{-6} \mu\text{b/sr}$ at 0° for incident proton momenta of 3–20 GeV/c . However, they point out that this is probably an underestimate of the cross section, since the form factors of nuclei at large momentum transfers may be much larger than those predicted by the oscillator shell model. For example, Domingo *et al.*⁴ reported observing at 1.22 GeV/c incident proton momentum the π^+ spectral peak from $^{12}\text{C}(p, \pi^+)^{13}\text{C}$ with $(d\sigma/d\Omega)_\phi \approx 0.5 \mu\text{b/sr}$. According to their analysis, this exceeds by a factor of 100 estimates made using harmonic oscillator wave functions.

The only relaxation of the large momentum transfer imposed by the kinematics of two-body final states occurs when the target mass becomes the same order of magnitude as the proton projectile mass. For example, in $p[p, K^+](p\Lambda)$, where it is assumed for the moment that $(p\Lambda)$ is a bound state, the momentum transfer between p and $(p\Lambda)$, as viewed in the $(p\Lambda)$ center-of-mass system, is $\geq 0.737 \text{ GeV}/c$. Indeed, a K^+ spectral peak corresponding to this reaction was observed by Melissinos *et al.*⁵ at incident proton momenta of 3.20 and 3.67 GeV/c with $(d\sigma/d\Omega)_{\text{c.m.}} \approx 0.25 \mu\text{b/sr}$ at 0° for both incident momenta. Since nuclear emulsion studies of hyperfragments have never identified a $(p\Lambda)$ hypernucleus, it is likely that the spectral enhancement for almost bound $p\Lambda$ states is due to the attractive $p-\Lambda$ final state interaction. These low relative momentum states are hereafter denoted $(p\Lambda)^*$.

The following sections give details of the experimental arrangement, π^+ and K^+ spectra observed at 0° from carbon, observation of the K^+ spectral peak from $p[p, K^+](p\Lambda)^*$, and upper limits on $(d\sigma/d\Omega)_\phi$ for π^+ and K^+ spectral peaks from carbon and other elements.

EXPERIMENTAL ARRANGEMENT

Protons having momenta of 1.8, 2.0, 2.5, 2.7, 2.89, and 3.1 GeV/c were provided by a resonantly

extracted external proton beam of the Lawrence Berkeley Laboratory Bevatron with intensities up to 5×10^{11} protons in a 1 sec spill. The proton momentum was calculated from the magnetic field and orbit radius during the flat-top portion of the magnet cycle with an estimated uncertainty of $\pm 2.0 \text{ MeV}/c$ in the absolute momentum. At the third focus of the septum external proton beam the protons impinged upon a target with typical dimensions 0.32 cm high \times 0.635 cm wide \times 12.7 cm long.

The target assembly contained three targets which could be moved into the same position in the proton beam. Typically, one target was polystyrene (chemically, CH) 12.7 cm long, a second target was carbon 7.87 cm long, the length being chosen for the same ionization energy loss as in the polystyrene, and a third carbon target 12.7 cm long was for use when K^+ counting rates were low. Polystyrene was used rather than polyethylene, which has twice as many hydrogen atoms, because of its better resistance to radiation-damage-induced changes of chemical composition.

The partially separated K^+ beam line for analysis and detection of secondaries emitted near 0° from the target is shown in Figs. 1 and 2. It had a vertical acceptance of $\pm 3 \text{ mrad}$ and a horizontal acceptance of $\pm 150 \text{ mrad}$. At the intermediate focus were placed vertical mass slits and horizontal slits defining a $\pm 2.5\%$ momentum acceptance. At approximately the center of the beam path from the intermediate to the final focus the beam was deflected vertically downward by 11.5° by magnet $M3$. This downward deflection vertically separated particles of differing momenta at the final focus to permit more precise momentum analysis by means of a 30 channel scintillation counter hodoscope. In order to minimize multiple scattering the beam was in vacuum up to the mass and momentum slits, in helium through magnet $M2$, and again in vacuum from the entrance of $Q6$ to the 30 channel hodoscope.

Utilizing a standard K^+ beam as a spectrometer required the experimenter to properly set, control, and monitor the currents in 10 magnets and in an electrostatic mass separator. The setting and monitoring of the regulated current supplies was manual during the major part of the running time when spectral line peaks were being examined or searched for. Toward the end of the experiment the setting and monitoring of the magnets and separator were brought under the control of a PDP-8 computer. Most of the data on K^+ and π^+ spectra were obtained with the beam under computer control.

Acceptable beam particles were defined by the coincidence $B = (S_1 \cdot S_3)_{\text{fast}} \cdot (S_2 \cdot S_4)_{\text{fast}} \cdot \bar{C}$, where the

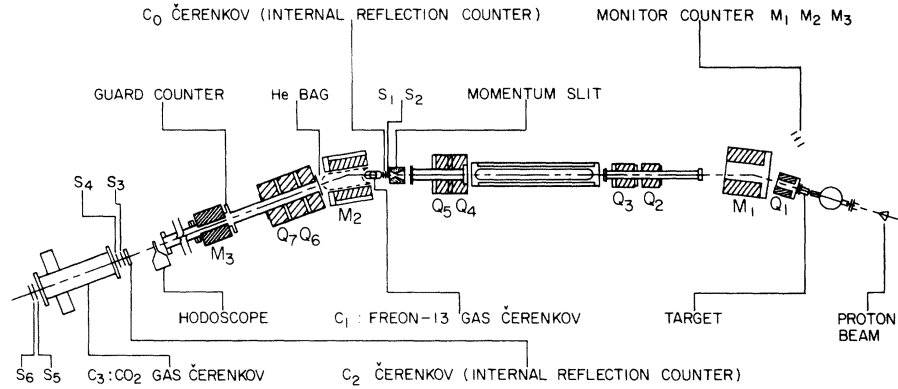


FIG. 1. Beam layout—plan view.

fast coincidences $(S_1 \cdot S_3)_{\text{fast}}$ and $(S_2 \cdot S_4)_{\text{fast}}$ had resolutions ≈ 2 ns full width at half maximum (FWHM) and were set for the appropriate K^+ or π^+ time of flight over the 12.8 m path. Scintillators S_1 and S_2 near the mass and momentum slits were 1.91 cm wide \times 1.27 cm high \times 0.32 cm thick. Scintillators S_3 and S_4 were 15.2 cm \times 15.2 cm \times 0.635 cm thick. Guard counter G , with a hole 5.1 cm high \times 10.2 cm wide, was mounted within the beam vacuum near M_3 . For some runs one or both of the counters S_5 and S_6 , each 20.3 cm in diameter, were also in the beam coincidence.

It was found that the separation provided by the electrostatic separator and the time-of-flight coincidences gave a clean K^+ signal when the target was bombarded with the full Bevatron energy, corresponding to an incident proton momentum of 5.74 GeV/c. However, for proton beams in the 2.5 to 3.1 GeV/c range, additional discrimination against pions and protons was needed. Discrimination against pions (and muons and elec-

trons) was provided by gas Čerenkov counters C_1 and C_3 in anticoincidence with the beam coincidence B . Čerenkov counter C_1 was 12.7 cm diam \times 61 cm long containing Freon 13 gas at 24 atm pressure, and was viewed by two RCA 8575 PM tubes, each independently viewing the Čerenkov radiation from 30 cm of the particle path.⁶ Counter C_3 was 20 cm diam \times 1.83 m long filled with CO_2 at 22 atm, and was viewed by two RCA 4522 PM tubes. Counter C_1 rejected pions with an inefficiency less than 4.4×10^{-4} ; counter C_3 , less than 1.1×10^{-3} . Counter C_1 was found to be sufficiently efficient in rejecting pions so that C_3 was not really needed; therefore, in order to increase counting rates, counters S_4 and S_5 were not included in the beam coincidence after C_1 was installed.

Discrimination against protons was provided by demanding a coincidence with Čerenkov counters C_0 and C_2 which contained 2.54 cm thick \times 56 cm long bars of UVA Plexiglas.⁷ The end of the bar

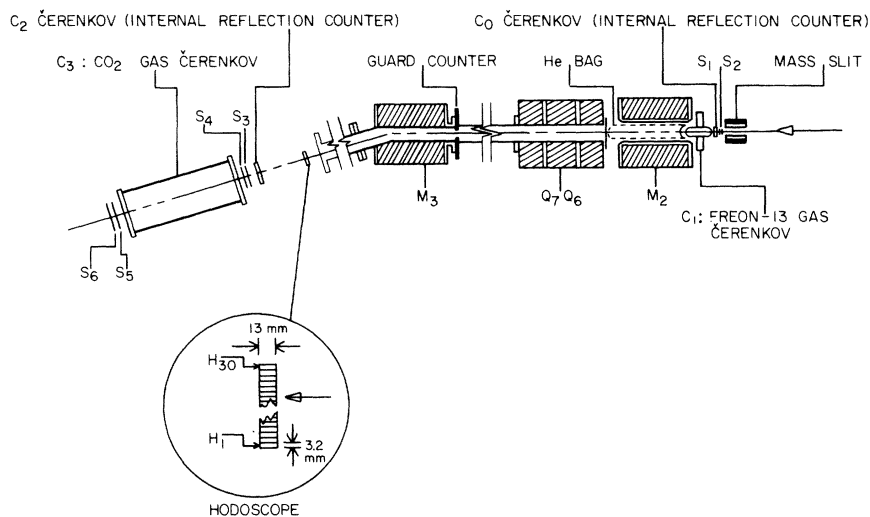


FIG. 2. Beam spectrometer—side elevation.

was viewed by a PM tube (RCA 8575 for C_0 , RCA 4522 for C_2), and the particles passed through the 2.54 cm thickness near the opposite end. If the Plexiglas bar was set at a suitable angle to the beam (90° for most runs), part of the Čerenkov light from kaons was emitted at sufficiently large angles to reach the PM tube via repeated total internal reflections, whereas the Čerenkov light from protons did not have the benefit of total internal reflection in attempting to reach the PM tube. These counters were each found to provide approximately a factor of 10 rejection of protons relative to kaons at 1.4 GeV/c beam momentum when the pulse height discriminator was set for 60% kaon detection efficiency.

Each channel of the 30 channel hodoscope consisted of a 10.2 cm wide \times 0.3175 cm high \times 1.27 cm thick (as viewed in the beam direction) plastic scintillator. Light pipes suitably bent and twisted conducted the light to individual RCA 6199 PM tubes.

To assist in normalizing beam counts to the number of protons interacting in the target, a three counter monitor telescope $M_1M_2M_3$ was set up in the target area which viewed particles emitted at approximately 45° from the target. Each scintillator was 1.27 cm diam \times 0.95 cm thick, and they were evenly spaced 10 cm apart. The $M = M_1 \cdot M_2 \cdot M_3$ coincidence rate was found by comparison with a secondary emission monitor in the external proton beam to be independent of incident proton energy in the 2.5–3.1 GeV/c range. Comparison of the monitor counting rates with C and CH targets indicated that the monitor counts could be attributed, within $\sim 5\%$ uncertainties, to proton interactions with the carbon nuclei. Hence, in taking data where CH–C differences were required in order to extract information on p – p collisions, runs with CH and C targets were taken for equal numbers of monitor counts.

CALIBRATION

After the K^+ beam was tuned for maximum flux and best K^+/π^+ separation at momentum settings of approximately 1.0, 1.2, 1.4, 1.6, and 1.8 GeV/c, absolute momentum settings were determined by observing the π^+ spectral peak from $p(p, \pi^+)d$ at incident proton momenta of 2.00, 2.50, 2.70, and 2.89 GeV/c with corresponding π^+ production momenta of 1.02, 1.45, 1.63, and 1.80 GeV/c. (Actual calculations of proton and pion momenta and of ionization energy losses in the targets and counters were carried out to tenths of MeV/c or better). A typical π^+ peak derived from the 30 channel hodoscope data for a pair of runs on CH and C targets at 2.50 GeV/c proton momen-

tum is shown in Fig. 3(a).

Since the acceptance of the beam falls off on either side of the central momentum, the counting rates of the 30 channel hodoscope are maximum in the central channels, and decrease to small values in the outer channels when observing a flat momentum spectrum. In order to correct the data for this response, it was found convenient to plot

$$f_i \equiv \frac{N_i(\text{CH}) - N_i(\text{C})}{N_i(\text{C})},$$

where $N_i(\text{CH})$ and $N_i(\text{C})$ are the numbers of counts in channel i from CH and C targets for the same number of monitor counts. The $d^2\sigma/d\Omega dp$ corresponding to f_i is then the cross section corresponding to $f_i[N_i(\text{C})]_{\text{max}}$ counts, where $[N_i(\text{C})]_{\text{max}}$ is the number of counts per channel at the peak of the hodoscope distribution observed from carbon. Since the CH–C differences are only used to observe spectral peaks from p – p collisions on top of a smooth background from p –C collisions, the results from this method of analyzing the data are insensitive to small mismatches in the number of p –C collisions in the CH and C runs. The distribution in Fig. 3(a) was calculated in this manner.

As a further check of the momentum calibration of the system, the Bevatron was adjusted to accelerate a very low intensity 1.80 GeV/c proton beam which came directly through the beam spectrometer also set at 1.8 GeV/c. The 30 channel hodoscope distribution is shown in Fig. 3(b). The main peak is due to protons which missed the target and entered the beam spectrometer without loss of energy. The smaller peak is attributable to protons which passed through the carbon target. The width of the distribution corresponds to a spectrometer resolution of 0.9% FWHM. The momentum calibration directly with 1.80 GeV/c pro-

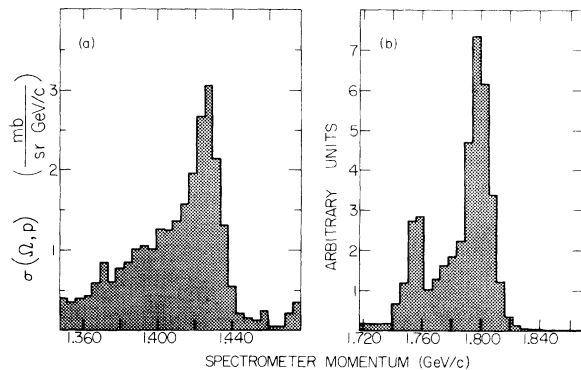


FIG. 3. (a) Typical $p(p, d)\pi^+$ peak. (b) Peaks from 1.800 GeV/c beam protons. Protons passing through the target form the left peak; protons missing the target form the central peak.

tons and with 1.80 GeV/c pions produced by 2.89 GeV/c protons differed by only 2.6 MeV/c, providing confirmation that proton momenta can be accurately calculated from the Bevatron parameters measured by the operating staff and that the system is stable and reproducible.

The potential utility of the $p(p, \pi^+)d$ line to relate beam counting rates to differential cross sections was diminished considerably by the fact that $(d\sigma/d\Omega)_0$ is poorly known for incident proton momenta in the 2.4–2.89 GeV/c range.^{8–12} Although the total cross section is smoothly decreasing through this region, the forward differential cross section in passing through an interference minimum. Also, the results of Overseth *et al.*⁹ and Dekkers *et al.*¹⁰ show that the shape of the angular distribution near 0° is rapidly changing in the 2.5–3.1 GeV/c incident proton momentum region, there being a sharp dip as 0° is approached for the lower end of this momentum range. This sharp dip makes the $(d\sigma/d\Omega)_0$ results of the previous experimenters, as well as the $p(p, \pi^+)d$ yields in this work, susceptible to large errors if the observed pions are not centered very close to 0°. Since $d\sigma/d\Omega$ is observed to be almost flat near 0° for a proton incident momentum of 2.824 GeV/c,¹⁰ the $p(p, \pi^+)d$ run at 2.89 GeV/c, with an average 2.872 GeV/c at the center of the target, has been used to calibrate the cross sections of this experiment, taking $(d\sigma/d\Omega)_{c.m.} = 8.7 \mu\text{b}/\text{sr}$. We were also guided in this choice by comparisons of π^+ rates in our data from CH and C targets, and also the results of Melissinos *et al.*¹³ on π^+ spectra at 32° produced by 3.67 GeV/c protons on hydrogen and carbon targets, which indicate that the π^+ production cross sections from p -C collisions are 5 to 7 times the corresponding ones for p -p collisions. Our π^+ spectra from p -C collisions would be expected to bear a similar relation to the π^+ spectra measured from 2.78 and 3.20 GeV/c p -p collisions by Reay *et al.*,¹¹ which they do with the above choice of cross section. A different choice of cross section normalization would affect all cross sections reported in this work by the same factor; the estimated uncertainty in the cross section normalization is $\pm 30\%$.

π^+ AND K^+ PRODUCTION SPECTRA AT 0° FROM CARBON

Since further theoretical work may provide more quantitative predictions relating cross sections for possible π^+ and K^+ spectral peaks to inclusive pion and kaon cross sections governed by the same matrix elements or intermediate states, π^+ and K^+ momentum spectra from proton-carbon collisions were explored for incident proton momenta of 2.50 and 2.70 GeV/c, and a few data points

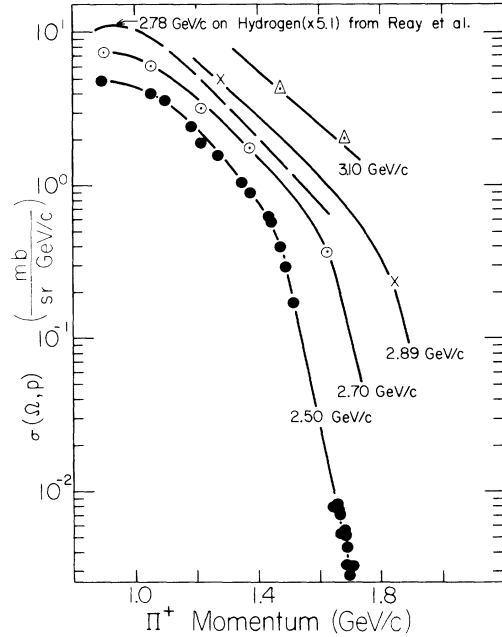


FIG. 4. π^+ laboratory spectra from carbon at 0° production angle.

acquired during the course of the line studies at 2.89 and 3.10 GeV/c are also reported. The π^+ spectra are shown in Figs. 4 and 5 and the K^+ spectra in Fig. 6.

The π^+ momentum spectra at 0° from carbon are almost the same in shape as the spectra from p - p collisions at similar incident momenta, as indicated by the curve in Fig. 4 from the results of Reay *et al.*¹¹ at 2.78 GeV/c. A more detailed pre-

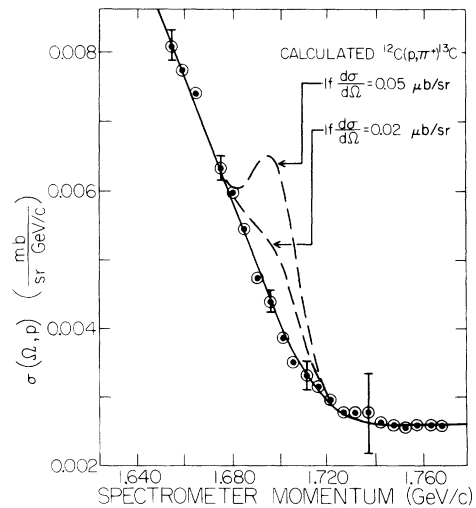


FIG. 5. Upper end of π^+ spectrum from 2.5 GeV/c protons on carbon. The dashed curves show the magnitudes of the spectral peaks expected for $^{12}\text{C}(p, \pi^+)^{13}\text{C}$ having $(d\sigma/d\Omega)_0 = 0.02, 0.05 \mu\text{b}/\text{sr}$.

resentation of the data at the upper end point of the π^+ spectrum from 2.50 GeV/c protons on carbon is shown in Fig. 5. There is no indication at this momentum of the spectral structure from $^{12}\text{C}(p, \pi^+)^{13}\text{C}$ reactions observed by Domingo *et al.*⁴ at 1.22 GeV/c incident proton momentum; the dashed curves show the expected shapes if $(d\sigma/d\Omega)_\phi$ were as large as 0.02 and 0.05 $\mu\text{b}/\text{sr}$, whereas they observed 0.5 $\mu\text{b}/\text{sr}$.

The K^+ momentum spectra at 0° from carbon are shown in Fig. 6 along with the spectrum from p - p collisions measured by Reed *et al.*¹⁴ at 3.20 GeV/c incident proton momentum. The p -C and p - p spectra are probably similar in shape except that no strong enhancement is observed near the upper end of the K^+ spectrum from carbon.

OBSERVATION OF $p[p, K^+](p\Lambda)^*$

The K^+ spectral peak first seen by Melissinos *et al.*⁵ from $p[p, K^+](p\Lambda)^*$ was reexamined both to confirm that our apparatus could detect such peaks and to see how the cross section varies for this reaction as the incident proton momentum becomes less. The data on the upper end of the K^+ spectrum at 0° from p - p collisions is shown in Figs. 7(a), and 7(b) for 2.89 and 3.10 GeV/c incident protons, respectively. Data was also taken at 2.70 GeV/c, where no significant difference between CH and C runs was observed. Since the plots involve a subtraction of C target data from CH target data, statistical fluctuations result in some bins with negative cross sections. At 2.89 GeV/c, some K^+ production above the background was observed;

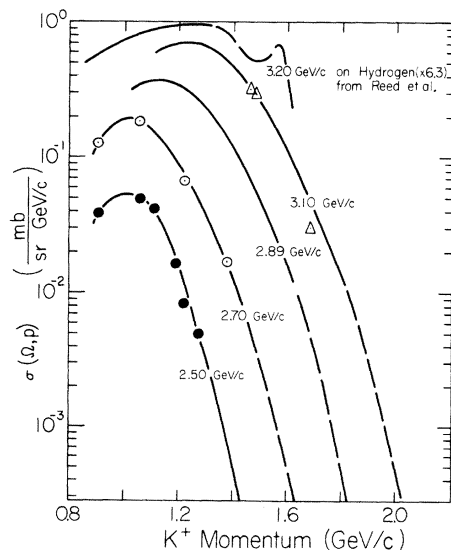


FIG. 6. K^+ laboratory spectra from carbon at 0° production angle.

at 3.10 GeV/c a clear peak was observed. The expected shift in position on the 30 channel hodoscope was observed when the beam momentum was raised 1.5%. In Fig. 7(b) the dashed curve shows the spectral shape to be expected near the maximum K^+ momentum if one multiplies phase space by a Goldberger-Watson (GW) final state enhancement factor¹⁵ for $p\Lambda$ effective range parameters $a = -1.9$ fm and $r_e = 3.0$ fm for both singlet and triplet states,¹⁶ and then folds in the spectrometer resolution. The GW formula has the form

$$\left(\frac{d^2\sigma}{d\Omega dp} \right)_{K^+, \phi} \propto \frac{d\sigma}{dQ} \propto \frac{(T+B)^2 T^{1/2}}{(T+A)^2 + T}, \quad (1)$$

where Q is the relative p - Λ kinetic energy, $T = (6.54)(10^{-3})r_e^2 Q$ with r_e in fm and Q in MeV, $A = -r_e/2a$, and $B = \frac{1}{4}[1 + (1 + 4A)^{1/2}]^2$. Although Eq. (1) has a complicated form, for a wide range of $p\Lambda$ effective range parameters Eq. (1) gives $d\sigma/dQ \approx$ constant, rapidly falling to zero for $Q < 1$ MeV.

The K^+ spectra observed by Melissinos *et al.*^{5, 14}

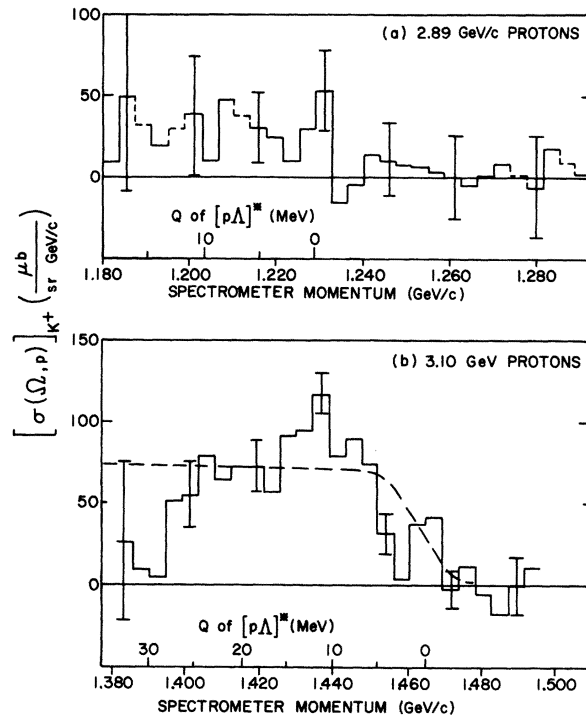


FIG. 7. (a) Upper end of K^+ spectrum from 2.89 GeV/c p - p collisions. (b) Upper end of K^+ spectrum from 3.10 GeV/c p - p collisions. The dashed curve shows the shape expected if effective range parameters $a = -1.9$ fm, $r_e = 3.0$ fm for both singlet and triplet p - Λ interactions are inserted in the Goldberger-Watson expressions for the spectral shape in the presence of a final state interaction.

TABLE I. Cross sections for K⁺ momentum spectrum peaks from p[p, K⁺](pΛ)*.

Incident proton momentum (GeV/c)	$\left(\frac{d^2\sigma}{d\Omega dp}\right)_{K^+, 0^\circ}$		$\left(\frac{d^2\sigma}{d\Omega^* dQ_{p\Lambda}}\right)_{K^+, 0^\circ}$	Reference
	$\left(\frac{\mu\text{b}}{\text{sr GeV}/c}\right)$		$\left(\frac{\text{nb}}{\text{sr MeV}/c}\right)$	
	ab	c.m.	c.m.	
2.70	<20	<3	<5	This work
2.89	29 ± 15	6 ± 3	7 ± 4	This work
3.10	86 ± 25	20 ± 6	22 ± 6	This work
3.26	103 ± 21	25 ± 5	26 ± 5	Ref. 14
3.67	92 ± 18	22 ± 4	21 ± 4	Ref. 14

at 3.20 and 3.67 GeV/c incident proton momenta and in this work at 3.10 GeV/c all show a definite peak near the upper end of the K⁺ spectrum which cannot be reproduced by the GW formula using effective range parameters which fit Λp elastic scattering and other hypernuclear data. Aaron and Amado¹⁷ have suggested that the GW assumption of slowly varying production amplitudes in the region of phase space near Q = 0 may not be justified, and that one must improve upon the GW formula. Unfortunately, accelerator scheduling limitations prevented further experimental study of the spectrum shown in Fig. 7(b).

The magnitudes of the K⁺ yields in the peak or shoulder at the upper end of the K⁺ momentum spectrum at 0° from p-p collisions are listed in Table I. The cross sections are given both with respect to laboratory and center-of-mass system variables. Although the yield cross section rises appreciably when changing from 2.89 to 3.10 GeV/c incident proton momentum, there is no further significant change in yield up to 3.67 GeV/c. (The threshold for p[p, K⁺](pΛ) is 2.34 GeV/c incident proton momentum.)

⁴Z(p, K⁺)^{A+1}Z_Λ AND ⁴Z(p, π⁺)^{A+1}Z CROSS SECTION UPPER LIMITS

Table II lists upper limits on $(d\sigma/d\Omega)_{\text{lab}}$ at 0° which result from the unsuccessful search for various hypothetical spectral peaks from reactions such as ¹²C(p, K⁺)¹³C_Λ, ¹²C(p, π⁺)¹³C, and similar reactions from Be and Fe at various incident proton momenta. The limit on observing a π⁺ line from ¹²C(p, π⁺)¹³C is set by estimating the minimum amount of spectral structure one would consider as an acceptable effect in the plot shown in Fig. 5.

The limits on the K⁺ lines were set by the level below which no clear K⁺ signal was discernible in the beam count. This limit also corresponded, in the best runs, to low counting rates (~10 counts/h). A K⁺ signal was checked by inserting either additional or less delay in the S₁ and S₂ counter signals to see if there was a peak or plateau in the region of delays appropriate for a K⁺ signal. Also, it was usually possible to arrange a brief Bevatron run with the full 5.74 GeV/c proton momentum either shortly before or after a series of K⁺ line

TABLE II. Cross section upper limits for π⁺ and K⁺ momentum spectrum peaks (1 nb = 10⁻⁹ b).

Reaction	Incident proton momentum (GeV/c)	Laboratory meson momentum (GeV/c)	90% confidence upper limit to $\left(\frac{d\sigma}{d\Omega}\right)_{\text{lab at } 0^\circ}$ (nb/sr)
¹² C(p, π ⁺) ¹³ C	2.50	1.704	20
d(p, K ⁺) ³ H _Λ	2.70	1.056	170
⁹ Be(p, K ⁺) ¹⁰ Be _Λ	2.50	1.418	11
¹² C(p, K ⁺) ¹³ C _Λ	2.50	1.438	2.8
¹² C(p, K ⁺) ¹³ C _Λ	2.70	1.635	600
¹² C(p, K ⁺) ¹³ C _Λ	2.89	1.818	84
⁵⁶ Fe(p, K ⁺) ⁵⁷ Fe _Λ	2.50	1.488	9

searches with identical beam and electronics settings to confirm that any K^+ 's would have been detected.

Immediately before and after each K^+ line search, the π^+ line from $p(p, \pi^+)d$ was examined to be sure all the beam magnets were properly set. Since these π^+ calibration lines had widths of 4–6 hodoscope channels (FWHM), the K^+ cross section limits were calculated from the number of counts in the appropriate 6 hodoscope channels centered on the expected K^+ line position. The uncertainty in K^+ line position is estimated to be ± 0.5 channels (± 2 MeV/c).

Most of the K^+ line searches were conducted with 2.50 GeV/c protons, looking for approximately 1.45 GeV/c K^+ 's, because the over-all performance of the K^+ beam was optimum at this momentum. At lower momenta, rate loss due to K^+ decays in flight became serious. At higher momenta, the K^+/π^+ and K^+/p discrimination of the electrostatic separator, time-of-flight coincidences, and internal-reflection Čerenkov counters rapidly deteriorated.

None of the cross section limits in Table II is in conflict with the predictions of Fetisov *et al.*,³ even if the K^+ cross section were 1000 times higher than their estimate based upon harmonic oscillator wave functions.

CONCLUSIONS

The π^+ spectra from proton-carbon collisions at 0° are very similar in shape to spectra from p - p collisions at the same incident proton momentum. The yields rise rapidly with increasing incident proton momentum in the 2.5–3.1 GeV/c region, roughly doubling for each 0.2 GeV/c increase of incident proton momentum. The K^+ yields from proton-carbon collisions at 0° rise even more rapidly in the 2.5–3.1 GeV/c range; roughly a factor of 5 for each 0.2 GeV/c increase of incident proton momentum.

The upper end of the K^+ momentum spectrum from p - p collisions at 3.10 GeV/c shows a peak clearly separated from the main, broad K^+ spectrum. An enhancement of the K^+ yield would be expected in the region of the observed peak due to the attractive p - Λ final state interaction. However, if the choice of effective range parameters favored by Λ - p elastic scattering and other hypernuclear data is employed in the Goldberger-Watson formula, only a shoulder would be expected at the upper end of the K^+ spectrum. An $n\Lambda$ enhancement at $Q = 33$ MeV was observed by

Cohn, Bhatt, and Bugg¹⁸; in our arrangement this would have been hidden in the K^+ background from many-body final states. The cross section for K^+ production near the upper end of the spectrum is roughly the same at 3.67, 3.20, and 3.10 GeV/c, but significantly less at 2.89 GeV/c and 2.70 GeV/c incident proton momentum. This K^+ peak or spectral enhancement appears to merit further study at a number of closely spaced intervals of incident proton momentum.

The cross section of $^{12}\text{C}(p, \pi^+)^{13}\text{C}$ falls at least a factor of 25 from 1.22 GeV/c, where it has been measured,⁴ to 2.50 GeV/c, where it was lost in background. Upper cross section limits have been placed on $^{12}\text{C}(p, K^+)^{13}\text{C}_\Lambda$ and similar reactions in Be and Fe which are 1000 times, or more, higher than presumably pessimistic theoretical estimates. Further improvement of the $^{12}\text{C}(p, \pi^+)^{13}\text{C}$ limit would require improved spectrometer resolution. Additional sensitivity to find the K^+ lines also would require some combination of more proton beam intensity, larger K^+ beam aperture, and shorter K^+ beam transport system to increase counting rates.

Concerning the possible use of $p(^AZ, ^{A+1}Z_\Lambda)K^+$ reactions in heavy ion beams to produce relativistic hypernuclei, these results indicate the production cross sections would be too low. Other reactions with three or more body final states are expected to have cross sections many orders of magnitude higher, mainly because the less constrained kinematics permit smaller momentum transfers.³

ACKNOWLEDGMENTS

The authors appreciate assistance from Professor E. W. Jenkins in tuning the K^+ beam and with the early runs, from Professor R. M. Kalbach for providing us with special tables of particle kinematics, from Dr. J. Brewer for assistance during the runs, from Professor F. A. Barnett and Professor P. H. Steinberg for loaning us their Freon 13 gas Čerenkov counter, and from Professor K. Hartt with helpful discussions. We are greatly indebted to Mr. Van Jacobson for writing the system computer programs to control and monitor the beam spectrometer magnets. We also are pleased to acknowledge the help and cooperation of Mr. Fred Lothrop and his Bevatron engineering and operating staff in setting up and running this experiment.

- *Work supported in part by National Science Foundation Grant No. MPS 70-02151.
- ¹L. Rosen (private communication). While our experiment was in progress, a proposal was submitted by another group to observe (p, K^+) reactions at LAMPF (G. Igo *et al.*, LAMPF Proposal No. 158).
- ²H. A. Grunder, W. D. Hartsough, and E. J. Lofgren, *Science* **174**, 1128 (1971); LBL Report No. 2090, October 1973 (unpublished).
- ³V. N. Fetisov, M. I. Koslov, and A. I. Lebedev, *Phys. Lett.* **38B**, 129 (1972).
- ⁴J. J. Domingo, B. W. Allardyce, C. H. Q. Ingram, S. Rohlin, N. W. Tanner, J. Rohlin, E. M. Rimmer, G. Jones, and J. P. Girardeau-Montaut, *Phys. Lett.* **32B**, 309 (1970).
- ⁵A. C. Melissinos, N. W. Reay, J. T. Reed, T. Yamanouchi, E. Sacharidis, S. J. Lindenbaum, S. Ozaki, and L. C. L. Yuan, *Phys. Rev. Lett.* **14**, 604 (1965). The same data are also discussed in Ref. 14.
- ⁶B. A. Barnett, P. F. Koehler, and P. H. Steinberg, U. of Maryland, Department of Physics Technical Report No. 894 (unpublished).
- ⁷It is important that the Plexiglas not scintillate; we first used ultraviolet-transmitting (UVT) Plexiglas, but the counter performed poorly, presumably because the plastic emitted scintillation light. The difference between suitable and unsuitable specimens can be seen under an ultraviolet lamp in a dark room.
- ⁸F. Turkot, G. B. Collins, and T. Fujii, *Phys. Rev. Lett.* **11**, 474 (1963).
- ⁹O. E. Overseth, R. M. Heinz, L. W. Jones, M. J. Longo, D. E. Pellett, M. L. Perl, and F. Martin, *Phys. Rev. Lett.* **13**, 59 (1964).
- ¹⁰D. Dekkers, B. Jordon, R. Mermod, C. C. Ting, G. Weber, T. R. Willitts, K. Winter, X. De Bouard, and M. Virargent, *Phys. Lett.* **11**, 161 (1964).
- ¹¹N. W. Reay, A. C. Melissinos, J. T. Reed, T. Yamanouchi, and L. C. L. Yuan, *Phys. Rev.* **142**, 918 (1966).
- ¹²H. L. Anderson, M. Dixit, H. J. Evans, K. A. Klare, D. A. Larson, M. V. Sherbrook, R. L. Martin, K. W. Edwards, D. Kessler, D. E. Nagle, H. A. Thiessen, C. K. Hargrove, E. P. Hincks, S. Fukui, *Phys. Rev. Lett.* **21**, 853 (1968); *Phys. Rev. D* **3**, 1536 (1971).
- ¹³A. C. Melissinos, T. Yamanouchi, G. G. Fazio, S. J. Lindenbaum, and L. C. L. Yuan, *Phys. Rev.* **128**, 2373 (1962).
- ¹⁴J. T. Reed, A. C. Melissinos, N. W. Reay, T. Yamanouchi, E. J. Sacharidis, S. J. Lindenbaum, S. Ozaki, and L. C. L. Yuan, *Phys. Rev.* **168**, 1495 (1968).
- ¹⁵M. L. Goldberger and K. M. Watson, *Collision Theory* (Wiley, New York, 1964), p. 550.
- ¹⁶R. H. Dalitz, in *Proceedings of a Conference on Nuclear and Hypernuclear Physics with Kaon Beams*, Brookhaven National Laboratory, July 1973 (unpublished), p. 1; M. Walsted, Ph.D. thesis, University of Rhode Island, 1974 (unpublished).
- ¹⁷R. Aaron and R. D. Amado, *Phys. Rev. Lett.* **31**, 1157 (1973); R. D. Amado, *Phys. Rev. Lett.* **33**, 333 (1974).
- ¹⁸H. O. Cohn, K. Bhatt, and W. M. Bugg, *Phys. Rev. Lett.* **13**, 668 (1964).

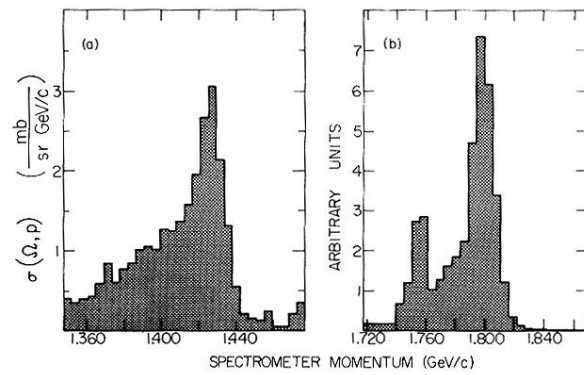


FIG. 3. (a) Typical $p(p, d)\pi^+$ peak. (b) Peaks from 1.800 GeV/c beam protons. Protons passing through the target form the left peak; protons missing the target form the central peak.